

PHYSIOLOGY AND REPRODUCTION

Ligusticum chuanxiong promotes the angiogenesis of preovulatory follicles (F1–F3) in late-phase laying hens

Hao Chen,* Xin Chen,* Zhenlei Ping,* Lixue Fang,* Xiaowen Jiang,* Ming Ge,* Jun Ma,* and Wenhui Yu *,†,‡,1

*College of Veterinary Medicine, Northeast Agricultural University, Harbin 150030, PR China; †Institution of Traditional Chinese Veterinary Medicine, Northeast Agricultural University, Harbin 150030, PR China; and ‡Key Laboratory of the Provincial Education Department of Heilongjiang for Common Animal Disease Prevention and Treatment, Harbin 150030, PR China

ABSTRACT *Ligusticum chuanxiong* (CX) is a traditional Chinese medicine that is widely planted throughout the world. CX is one of the most important and commonly used drugs to enhance blood circulation. The preovulatory follicles in laying hens have a large number of blood arteries and meridians that feed the follicles' growth and maturation with nutrients, hormones, and cytokines. With the extension of laying time, preovulatory follicles angiogenesis decreased gradually. In this study, we studied the mechanism of CX on preovulatory follicles angiogenesis in late-phase laying hens. The results show that CX extract can increase the angiogenesis of preovulatory follicles (F1–F3) of late-phase laying hens. CX extract can promote vascular endothelial

growth factor receptor 2 (VEGFR2) phosphorylation in preovulatory follicles theca layers, promote the proliferation, invasion and migration through PI3K/AKT and RAS/ERK signaling pathways in primary follicle microvascular endothelial-like cells (FMECs). In addition, CX extract can up-regulate the expression of hypoxia inducible factor α (HIF1 α) in granulosa cells (GCs) and granulosa layers through PI3K/AKT and RAS/ERK signaling pathways, thereby promoting the secretion of vascular endothelial growth factor A (VEGFA). In conclusion, the current study confirmed the promoting effect of CX extract on the preovulatory follicles angiogenesis, which sets the stage for the design of functional animal feed for late-phase laying hens.

Key words: *Ligusticum chuanxiong*, preovulatory follicles, angiogenesis, late-phase laying hens

2023 Poultry Science 102:102430

<https://doi.org/10.1016/j.psj.2022.102430>

INTRODUCTION

The abundant blood vessel network is the prerequisite for follicle development in laying hens (Ma et al., 2020). As the follicle develops, blood vessels and innervation reach the follicle through the pedicle and radiate through theca layer. Passive diffusion from stromal blood arteries supplies sufficient nutrition and oxygen to primary follicles (Robinson et al., 2009). However, for follicles to develop through these phases, a distinct capillary network must exist surrounding each one. During the process of follicles development, it is restricted to the theca layer and does not affect the granulosa layer, which is avascular (Tamanini and De Ambrogi (2004). When primary follicles are selected to the preovulatory

hierarchy, preovulatory follicles begin to grow rapidly from about nine mm in diameter to more than 40 mm in a few days (Scanes et al., 1982). With the increase of follicle size and ovulation time, the percentage of blood flow to the 5 largest preovulatory follicles, which had the greatest blood flow, got increasing within the fully developed ovary. The preovulatory follicles have a large number of blood arteries and meridians that feed the follicles' growth and maturation with nutrients, hormones, and cytokines (Nalbandov and James (1949). However, studies have shown that ovaries age earlier than other organs (Zhang et al., 2019). With the extension of laying time, the thickness of late-phase laying hens granular layer and theca layer decrease (Hao et al., 2021). Therefore, increasing the blood flow to the preovulatory follicles of late-phase laying hens and extending the period of high-quality laying hens have drawn increased attention.

The dried rhizome of *Ligusticum chuanxiong* Hort is known as Chuanxiong Rhizome (CX) (Chen et al., 2018). In the therapeutic application of TCM, CX is one

© 2022 The Authors. Published by Elsevier Inc. on behalf of Poultry Science Association Inc. This is an open access article under the CC BY-NC-ND license (<http://creativecommons.org/licenses/by-nc-nd/4.0/>).

Received October 12, 2022.

Accepted December 13, 2022.

¹Corresponding author: yuwenhui@neau.edu.cn

of the most significant and often used medications for enhancing blood circulation. CX is often used either alone or in connection with other pharmaceutical substances. From this plant, over 170 chemicals have been extracted and identified. Phthalides, terpenes, enols, polysaccharides, alkaloids, organic acids, and esters are the major active ingredients in CX (Pu et al., 2022). Ligustrazine, Ferulic acid, Isovanillin, Senkyunolide A, Ligustilide, and Levistilide A are the primary bioactive elements of CX (Yan et al., 2005; Liu et al., 2014). Due to its unique efficacy, CX is frequently used in the prevention and treatment of many ailments, including cardiovascular/cerebrovascular disorders and gynecological diseases. (Lim et al., 2006; Yang et al., 2010; Dong et al., 2020; Tang et al., 2021). According to earlier research, Ligustilide increases the permeability of the blood-brain barrier through the HIF1 α /VEGF signaling pathway, Ligustrazine promotes peritoneal angiogenesis by modulating the VEGF/HIPPO/YAP signaling pathway, and Ferulic acid controls angiogenesis through VEGFA (Lin et al., 2010; Wu et al., 2019; Zhu et al., 2021). Instead of focusing on one particular process, CX may include several active substances that work in concert to effectively promote angiogenesis. However, the precise processes of these active ingredients are still unclear.

Both angiogenesis, the process of creating new blood vessels, and vascularogenesis, the process of creating blood vessels from scratch from endothelial cells, are essential for development and eventual physiologic balance (Apte et al., 2019). Over 25 yr ago, the vascular endothelial growth factor A (VEGFA), a crucial component of angiogenesis, was discovered, isolated, and cloned (Uemura et al., 2021). Due to its crucial function in controlling angiogenesis both in health and illness, VEGFA receives the majority of attention. The VEGF signaling pathway, however, is complex and has a number of ligand-receptor interactions that control many activities in various cell types in a context-dependent manner (Uemura et al., 2021). Vascular endothelial growth factor receptor 2 (VEGFR2) is a VEGFA receptor that is highly homologous to VEGFA. VEGFA ligands bind to both VEGFR1 and VEGFR2, however VEGFR2 is the main receptor used for signaling, which promotes endothelial cell migration, proliferation, and survival as well as increases vascular permeability (Peach et al., 2018). Hypoxia inducible factor α (HIF1 α) is a key regulator of VEGFA expression. Epidermal growth factor (EGF), platelet-derived growth factor (PDGF) and other hypoxia regulated genes, as well as HIF1 α , co-ordinate VEGFA production (Semenza, 2014).

As a result, this study examined how CX extract affected the angiogenesis of preovulatory follicles (F1–F3) in late-phase laying hens. Subsequently, we investigated the constituents and targets of CX extract and created a network of proteins that CX extract works on as angiogenesis targets after detecting the active components in CX extract using LC-MS. Finally, molecular docking and in vivo/vitro experiments verified the key targets of CX extract in promoting angiogenesis. Our findings demonstrated that CX extract might enhance

the angiogenesis of preovulatory follicles in late-phase laying hens, up-regulate the phosphorylation level of VEGFR2 in the theca layers and FMECs, and stimulate the secretion of VEGFA in the granulosa layers and GCs.

MATERIALS AND METHODS

Ethics Statement

Animal care in this study was performed in accordance with the Animal Experiment Management Regulations (Ministry of Science and Technology of China, 2004) approved by the Animal Care and Use Committee of Northeast Agricultural University, China.

Preparation of Ethanol Extract of CX

The air-dried herbs Ligusticum chuanxiong Hort used in this study were purchased from a Chinese herbal medicine company (Sichuan, China), identified by professors from institute of Chinese Veterinary Medicine, Northeast Agricultural University. Took 100 g of dried CX ground into powder by a herb grinder. The powder was extracted three times with 1L of 75% ethanol. Then the extracted solution was filtered to remove insoluble materials and freeze-dried at -50°C . The average yield of CX was 16.8% (W/W). The freeze-dried was stored at -80°C . Before being administered to the chicken or cells, the extract was dissolved in distilled water or DMEM.

Animals and Treatment

A total of 50 Hy-line Brown laying hens were selected at age of 30 wk (N = 10) and 70wk (N = 40). All chicken were maintained in individual cages (400 mm \times 380 mm \times 360 mm), and lived in standard conditions (temperature at $23 \pm 2^{\circ}\text{C}$, relative humidity at $60 \pm 10\%$ and 16:8 h light/dark cycle). Water and diets were available ad libitum. Experiments were performed after the chicken acclimatized to laboratory conditions for one week. The 71 wk laying hens were randomly divided into 4 groups (N = 10): control group, low concentration of CX extract treatment group, medium concentration of CX extract treatment group and high concentration of CX extract treatment group. The 31 wk laying hens were set as a positive control group (N = 10). The laying hens in the control group and the positive control group were provided with a normal diet for 4 wk. In addition to their normal diet, the low, medium, and high concentration CX extract treatment groups received 1 g/d, 2 g/d, and 4 g/d of CX extract, respectively. At 35 wk and 75 wk of age, all chickens were euthanized 3 h after egg laying and preovulatory follicles (F1–F3) were harvested.

LC-MS

CX extract (100 mg) were individually grounded with liquid nitrogen and the homogenate was resuspended with prechilled 80% methanol by well vortex. The samples were

incubated on ice for 5 min and then were centrifuged at 15,000 g, 4°C for 20 min. Some of supernatant was diluted to final concentration containing 53% methanol by LC-MS grade water. The samples were subsequently transferred to a fresh Eppendorf tube and then were centrifuged at 15,000 g, 4°C for 20 min. Finally, the supernatant was injected into the LC-MS/MS system analysis

LC-MS/MS analyses were performed using an ExionLC AD system (SCIEX) coupled with a QTRAP 6500+ mass spectrometer (SCIEX). Samples were injected onto a Xselect HSS T3 (2.1 × 150 mm, 2.5 μm) using a 20-min linear gradient at a flow rate of 0.4 mL/min for the positive/negative polarity mode. The eluents were eluent A (0.1% Formic acid-water) and eluent B (0.1% Formic acid-acetonitrile). The solvent gradient was set as follows: 2% B, 2 min; 2 to 100% B, 15.0 min; 100% B, 17.0 min; 100-2% B, 17.1 min; 2% B, 20 min. QTRAP 6500+ mass spectrometer was operated in positive polarity mode with Curtain Gas of 35 psi, Collision Gas of Medium, Ion Spray Voltage of 5,500 V, Temperature of 550°C, Ion Source Gas of 1:60, Ion Source Gas of 2:60. QTRAP 6500+ mass spectrometer was operated in negative polarity mode with Curtain Gas of 35 psi, Collision Gas of Medium, Ion Spray Voltage of -4,500 V, Temperature of 550°C, Ion Source Gas of 1:60, Ion Source Gas of 2:60.

Target Prediction

The customary SMILE formats of selected compounds were acquired from the PubChem database (<https://pubchem.ncbi.nlm.nih.gov>). The targets of active compounds in CX extract were predicted by Super-PRED (<https://prediction.charite.de>). Furthermore, significant targets of angiogenesis were obtained from GeneCards (<https://www.genecards.org>). Intersection of the targets which were predicted by Super-PRED and the targets of angiogenesis were taken. Used Uniprot (<https://www.uniprot.org/>) to convert overlapping targets into UniProt ID. The protein-protein interaction (PPI) analysis was performed by STRING (<https://cn.string-db.org/>) and the combined score was greater than or equal to 0.7. Cytoscape 3.9.1 was used to visualize the network of overlapping targets.

GO and KEGG Pathway Enrichment Analysis

The targets were imported into Metascape (<https://metascape.org/gp/index.html#/main/step1>) to perform Gene Ontology (GO) enrichment analysis and Kyoto Encyclopedia of Genes and Genomes (KEGG) pathway enrichment analysis. GO Molecular Functions, GO Biological Processes and GO Cellular Components were downloaded. The results were presented as bar plot and bubble plot.

Molecular Docking

Three-D structure of compounds downloaded from PubChem. The initial 3-dimensional geometric

coordinates of the X-ray crystal structure were downloaded from the Protein Databank (<https://www.rcsb.org/>). Perform the molecular docking with AutoDock Vina. The protein-ligand interaction with the highest score was selected to analyze the results using PyMol and Discovery Studio.

Isolation and Culture of FMECs and GCs

We have successfully isolated primary GCs and FMECs from chicken preovulatory follicles according to the previously described methods (Chen et al., 2022a). Briefly, hens aged 30 wk which laying rate was more than 90% were used in this study. Hens were euthanized, preovulatory follicles (F1–F3) were moved out. A scalpel was used to release the yolk, and then separate granulosa layers and theca layers. The granulosa layers were put into 1 mg/mL type II collagen (Solarbio, Beijing, China) and digested at 37°C water bath for 8 min. M199 (HyClone, Logan, UT) was supplemented with 10% FBS (Clark Bioscience, Virginia) was added, filtered through nylon mesh (70 μm) and then centrifuged. The pellet was resuspended in M199 (containing 10% FBS and 1% penicillin-streptomycin) and the granulosa cells were cultured at 37°C under 5% CO₂. Theca layers were digested in DPBS containing 1 mg/mL type I collagenase (Solarbio, Beijing, China), 0.4 mg/mL DNase (Solarbio, Beijing, China) and 0.1% BSA (Solarbio, Beijing, China) at 37°C water bath for 60 min. DMEM (HyClone, Logan, UT) was supplemented with 10% FBS was added, filtered through nylon mesh (70 μm) and then centrifuged. Meanwhile, precooled 35% Percoll (Solarbio, Beijing, China) was centrifuged at 30,000 g at 4°C for 15 min. The pellet was resuspended in DMEM and tiled on the centrifuged Percoll. After centrifuging for 15 min at 400 g in a vertical centrifuge, the solution was divided into 3 layers. Cells in the middle layer (a density of 1.033–1.047 g/mL) were absorbed into a 15 mL centrifuge tube, and centrifuged. The pellet was resuspended in DMEM (containing 10% FBS, 50 μg/mL ECGs [Sigma-Aldrich, St. Louis] and 1% penicillin-streptomycin [Sigma-Aldrich, St. Louis]) and follicle microvascular endothelial-like cells were cultured at 37°C under 5% CO₂. The third to sixth generations of FMECs were used for experiments.

Cells Activity Assay

FMECs and GCs cells were cultured in 96-well plates treated with different concentrations (25, 50, 100, 200, 400 μg/mL) of CX for 24 h or 48 h. Removed the medium and cck-8 (Solarbio, Beijing, China) was added to each well and incubated for 2 h at 37°C. Used full wavelength microplate reader (Bio Tek, Vermont) measure the absorbance at 450 nm.

Morphological Observation

As previously (Chen et al., 2022b), preovulatory follicles were fixed in 4% paraformaldehyde for 24 h at 4°C.

The paraffin sections were prepared and then H.E. staining were carried out. H.E. sections of preovulatory follicles were observed using upright light microscope and imaged by Nikon imaging workstation (Nikon, Tokyo, Japan).

Immunofluorescence

FMECs and GCs were fixed with 4% paraformaldehyde, permeabilized with 0.25% triton X-100. After blocking with FBS, cells were incubated with primary antibodies, Alexa Fluor 594 (red) or Alexa Fluor 488 (green) (ABclonal, Wuhan, China) conjugated second antibodies and DAPI (blue) (Solarbio, Beijing, China). Paraffin-embedded preovulatory follicles were sectioned, dewaxed, antigen repair and incubated with primary antibodies, Alexa Fluor 594 (red) or Alexa Fluor 488 (green) conjugated second antibodies and DAPI (blue). Images were acquired using fluorescence microscopy (Nikon, Tokyo, Japan). The primary antibodies in IF are as follows: CD31 (1:100), VEGFA (1:100), VEGFR2 (1:100), P-VEGFR2 (1:100), HIF1- α (1:100) (ABclonal, Wuhan, China).

ELISA

The GCs (5×10^5 cells/mL) treated with different concentrations of CX (100 and 200 $\mu\text{g}/\text{mL}$) were seeded in plates for 48 h at 37°C. Cell media were harvested in sterile tubes and centrifuged (12,000 rpm, 10 min, 4°C) to obtain the supernatants. VEGFA ELISA kit was purchased from Nanjing Jiancheng Bioengineering Institute (Jiancheng, Nanjing, China). The target protein concentrations were detected by the method consistent with the manufacturer's instructions.

Western Blot

Preovulatory follicles, FMECs and GCs were lysed in RIPA lysis buffer containing combined protease and phosphatase inhibitors to extract total proteins. The content of proteins was determined using BCA kit (Solarbio, Beijing, China). All the samples were resolved on SDS-PAGE of gradient concentration and transferred to polyvinylidene difluoride membranes. After blocking, membranes were incubated with primary antibodies for the detection of CD31 (1:1000), VEGFA (1:500), VEGFR2 (1:1000), P-VEGFR2 (1:500), HIF1- α (1:1000), p-PI3K (1:500), PI3K (1:1000), p-AKT (1:500), AKT (1:1000), p-MTOR (1:500), MTOR (1:500), p-P70S6K (1:500), P70S6K (1:500), RAS (1:500), RAF (1:500), p-MEK (1:500), MEK (1:500), p-ERK (1:500), ERK (1:500), MMP2 (1:500), MMP9 (5:100), and β -actin (1:1000) and secondary antibodies (ABclonal, Wuhan, China). Protein bands were visualized with chemiluminescent system (Tanon, Shanghai, China) and quantified by Image J software.

Wound Healing Assay

Full confluency of the 5×10^5 cells/mL FMECs was achieved in the 6-well plate and began to scratch. After using a sterile pipette tip scratch, cell debris were removed with PBS. The medium was added with different CX concentrations (100 and 200 $\mu\text{g}/\text{mL}$). After cultured in 37°C for 6 h and 12 h, images were taken under a microscope (Nikon, Tokyo, Japan).

Transwell Invasion Assay

The Matrigel (Corning, Bedford) was spread over $8\mu\text{m}$ pore size polycarbonate filter with a diameter of 24 wells (Corning, Bedford). ECG medium was added into the lower compartment. The FMECs (2×10^5 cells/mL) were cultured in the medium with different concentrations of CX (100 and 200 $\mu\text{g}/\text{mL}$) for 24 h. We fixed FMECs podocytes in 4% paraformaldehyde, stained with 0.1% crystal violet, and then permeabilized them. Finally, a microscope was used to take pictures and analyzed by Image J.

Tube Formation Assay

The Matrigel was spread over 48 wells in advance and cultured in 37°C for 30 min. The first experiment, FMECs (2×10^5 cells/mL) that treated by different concentrations of CX (100 and 200 $\mu\text{g}/\text{mL}$) were seeded in Matrigel pretreated plates and cultured at 37°C for 6 h. The second experiment, GCs (5×10^5 cells/mL) which treated with different concentrations of CX (100 and 200 $\mu\text{g}/\text{mL}$) were seeded in plates for 48 h at 37°C. Absorb GCs medicated medium and add them into FMECs which were seeded in Matrigel pretreated plates. The plates were cultured at 37°C for 6 h. The tube formation state was observed by a microscope and analyzed by Image J.

Statistical Analysis

The data were analyzed and visualized using Graph-Pad Prism (version 8, San Diego). The values were presented as mean \pm S.E.M. Comparisons among the groups were evaluated using one way ANOVA with Tukey test. P value < 0.05 was considered statistically significance of difference.

RESULTS

LC-MS

As shown in [Figure 1A](#) and [1B](#), 12 compounds were characterized by LC/MS, including 1 Ligustrazine ($m/z = 136.19$; $rt = 0.88$ min), 2 D-Arabitol ($m/z = 152.15$; $rt = 0.926$ min), 3 Isoleucine ($m/z = 13.17$; $rt = 2.11$ min), 4 Folic acid ($m/z = 441.4$; $rt = 5.117$ min), 5 Caffeic acid ($m/z = 180.16$; $rt = 5.801$ min), 6 Sodium ferulate ($m/z = 216.17$; $rt = 6.81$ min), 7 Ferulic acid ($m/z = 194.19$; $rt = 6.881$ min), 8 Isochlorogenic acid A ($m/z = 194.19$; $rt = 6.881$ min).

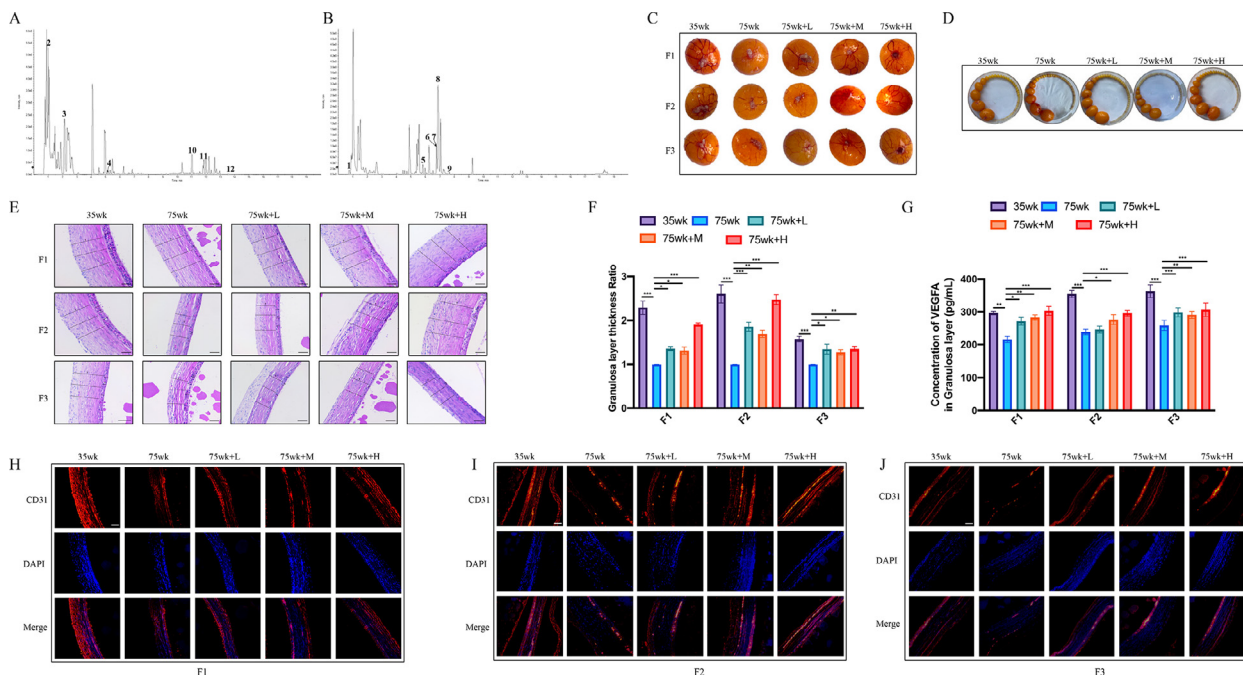


Figure 1. Compounds characterization of CX extract and dose-dependent effects of CX extract on angiogenesis of preovulatory follicles. Based peak intensity chromatograms of CX extract acquired by LC-MS, (A) positive mode and negative (B). (C) Blood vessel was observed on surface of preovulatory follicles (F1–F3) after CX extract treated. (D) Number of follicles in each group after treatment with CX extract. (E) HE staining to detect the granulosa layers thickness after CX extract treated. Scale bar = 100 μ m. (F) Histogram of granulosa layer thickness ratio. (G) Elisa analysis of VEGFA concentration in granulosa layer (F1–F3) after treatment by CX extract. Immunofluorescence staining of CD31 in CX extract-treated preovulatory follicles, (H) F1, (I) F2, and (J) F3. Scale bar = 100 μ m. All experiments were performed in triplicate, and the data are the mean \pm S.E.M (* P < 0.05, ** P < 0.01, *** P < 0.001).

$z = 516.45$; $rt = 6.912$ min), 9 Isovavillin ($m/z = 152.15$; $rt = 7.676$ min), 10 Senkyunolide A ($m/z = 192.25$; $rt = 10.97$ min), 11 Ligustilide ($m/z = 190.23$; $rt = 11.86$ min), 12 Levistilide A ($m/z = 380.48$; $rt = 13.75$ min). The CX extract indicated that the sample used in this experiment contained the active ingredients described in previous research (Li et al., 2021).

CX Extract Promotes Angiogenesis in Preovulatory Follicles of Late-phase Laying Hens

We investigated angiogenesis in preovulatory follicles of CX extra at different doses in 35 wk and 75 wk laying hens in vivo. As Figure 1C shown, the preovulatory follicles (F1–F3) of 35 wk laying hens had a large number of blood vessels distributed on the surface. However, there were a few blood vessels distributed on F1 to F3 in 75 wk late-phase laying hens. After feeding CX extract for 4 wk, the blood vessels were distributed on the surface of F1 to F3 in groups 75 wk + L, 75 wk + M and 75 wk + H was more than in group 75 wk. And we found that the number of follicles in groups 75 wk + L, 75 wk + M, and 75 wk + H was more than that in group 75 wk (Figure 1D). We used histopathological methods to explore the effects of CX extract on preovulatory follicles with angiogenesis (Figure 1E, F). HE staining showed that the granulosa layers of F1 to F3 at 35 wk were thicker than those at 75 wk ($P < 0.001$) and the granulosa cells were closely arranged. Compared with 75 wk,

the granulosa layer in treatment groups had different degrees of thickening ($P < 0.05$, $P < 0.01$, and $P < 0.001$). Therefore, we quantitatively determined the degree of concentration of VEGFA in granulosa layer by Elisa (Figure 1G). Elisa showed that, concentration of VEGFA in granulosa layer of F1 to F3 at 35 wk was higher expression than that at 75 wk ($P < 0.01$ and $P < 0.001$). Compared with 75 wk, concentration of VEGFA in treatment groups had higher expression ($P < 0.05$, $P < 0.01$, and $P < 0.001$). The CD31 protein is a blood vessel maker. From IF staining (Figure 1H–J), CD31 was mainly located in theca layers. As IF staining showed, the expression of CD31 in F1 to F3 at 35 wk groups was higher than that at 75 wk. After CX extract administration, the expression levels of CD31 were up-regulated in F1 to F3 treatment groups.

Network Pharmacology Analysis

The structural formulas of the twelve components validated by LC-MS are shown in Figure S1. Their predicted targets added up to 191 by employing SuperPRED. Intersecting 191 prediction targets with 1,263 angiogenesis targets, 51 targets were obtained. Therefore, 12 ingredients of CX extract and 51 angiogenesis targets were used for further analysis. The PPI data analyzed via String was imported to Cytoscape to perform network analysis, and the size of the nodes was proportional to the degree of centrality obtained from topology analysis (Figure 2A). Topology analysis indicated that

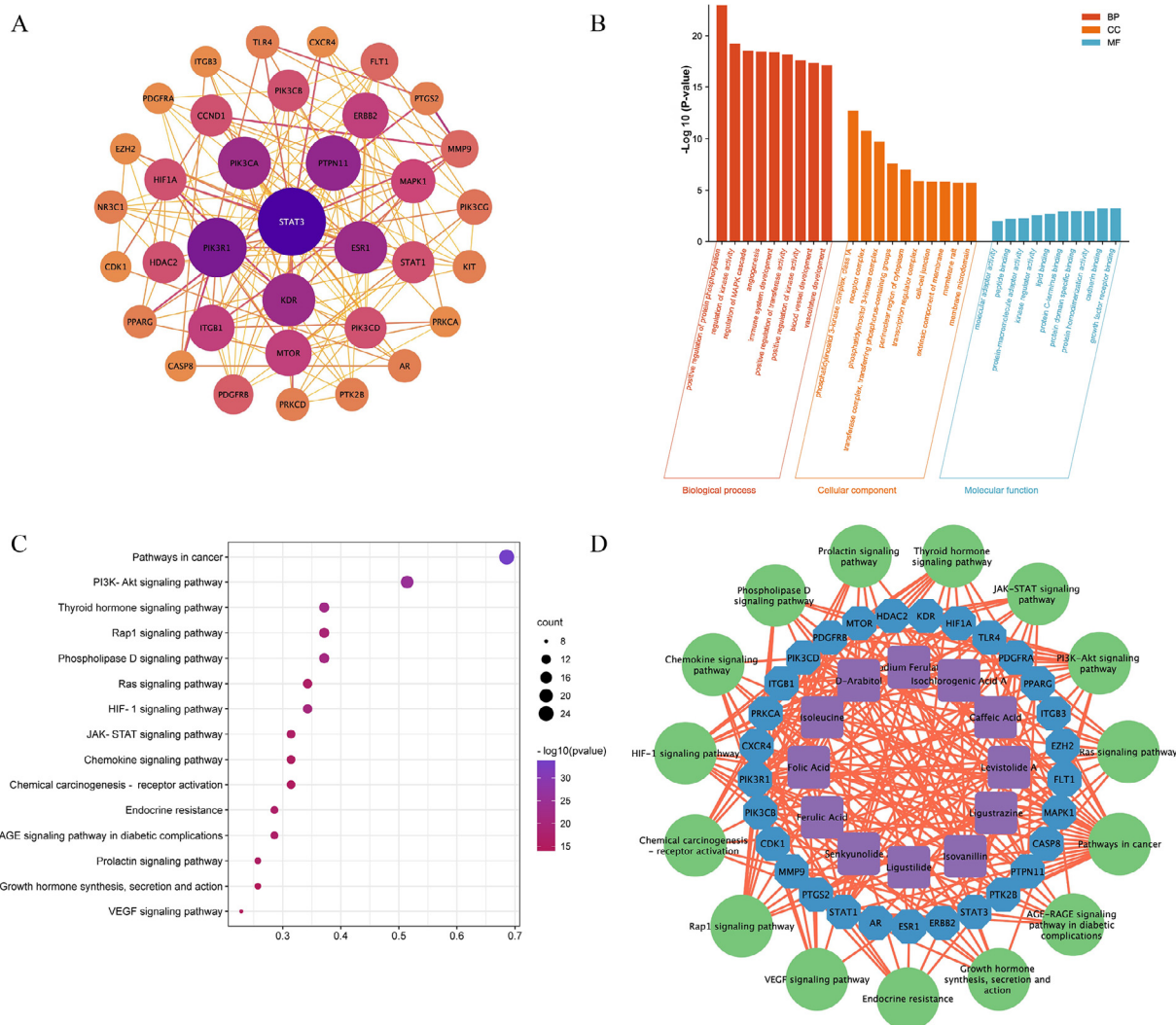


Figure 2. Network pharmacology analysis of twelve validated constituents of CX extract. (A) PPI results. (B) GO enrichment results. (C) KEGG pathway enrichment results. (D) Component-target-pathway network of CX extract in effect in angiogenesis.

STAT3, PIK3R1, PTPN11, KDR (VEGFR2), PIK3CA, ESR1, ERBB2, ITGB1, MTOR, MAPK1, CCND1, HDAC2, STAT1, HIF1 α , PIK3CD were the top 15 shared targets from the perspective of degree centrality. GO analysis in Metascape was performed to further investigate the biological functions of CX extract on angiogenesis. GO enrichment analysis indicated that these targets primarily existed in receptor complex, transferase complex, transferring phosphorus-containing groups, perinuclear region of cytoplasm, transcription regulator complex, cell-cell junction and were involved in positive regulation of protein phosphorylation, regulation of kinase activity, angiogenesis and other biological processes. The principal molecular functions of CX extract that promoted angiogenesis were molecular adaptor activity, peptide binding, protein-macromolecule adaptor activity, kinase regulator activity (Figure 2B). To further prove the mechanism of CX extract promoting angiogenesis, KEGG pathway enrichment analysis was conducted on the targets by ClusterProfiler package. As Figure 2C shows, the key pathways associated with angiogenesis were PI3K-AKT signaling pathway, Ras signaling pathway, HIF-1 α signaling pathway, JAK-STAT

signaling pathway and VEGF signaling pathway. We constructed a network of components, targets and enriched KEGG pathways (Figure 2D). The network clarifies that a component can act on multiple pathways or multiple targets, and a target may be related to multiple pathways or multiple components.

Molecular Docking Verification

We analyzed the potential molecular mechanisms of the CX extract active components in angiogenesis using bioinformatics (Figure 3). Through target prediction analysis, possible targets for the compounds were obtained. We determined that HIF1 α and VEGFR2 proteins might be potential targets of CX extract active components, and the components might promote angiogenesis. Multiple amino acid residues in HIF1 α protein interact with active components: the interaction energy of Caffeic acid and HIF1 α protein was -6.1 kcal/mol, the interaction energy of Ferulic acid and HIF1 α protein was -6.2 kcal/mol, the interaction energy of Ligustilide and HIF1 α protein was -7.2 kcal/mol, the interaction

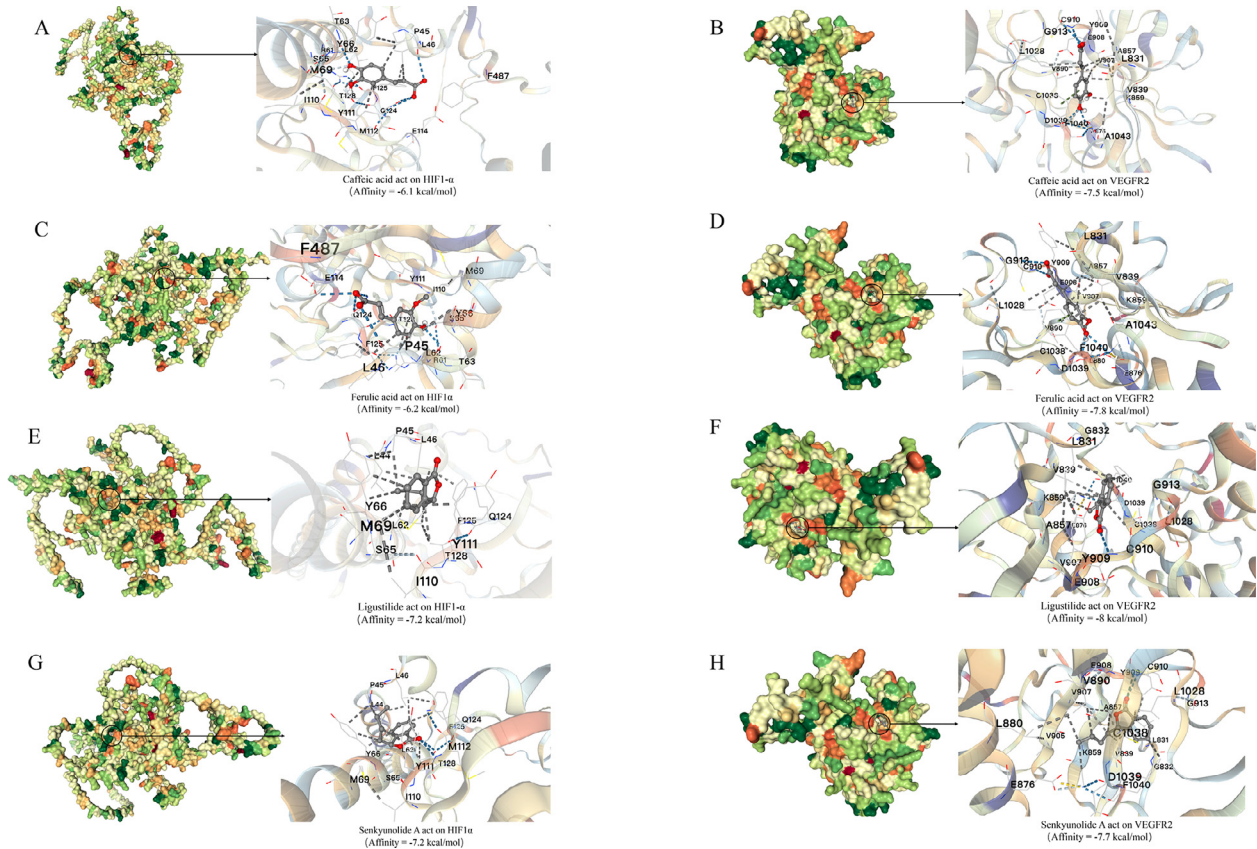


Figure 3. Demonstration of molecular docking of drugs and genes. (A) Demonstration of molecular docking of Caffeic acid and HIF1 α . (B) Demonstration of molecular docking of Caffeic acid and VEGFR2. (C) Demonstration of molecular docking of Ferulic acid and HIF1 α . (D) Demonstration of molecular docking of Ferulic acid and VEGFR2. (E) Demonstration of molecular docking of Ligustilide and HIF1 α . (F) Demonstration of molecular docking of Ligustilide and VEGFR2. (G) Demonstration of molecular docking of Senkyunolide A and HIF1 α . (H) Demonstration of molecular docking of Senkyunolide A and VEGFR2.

energy of Senkyunolide A and HIF1 α protein was -7.2 kcal/mol. Multiple amino acid residues in VEGFR2 protein interact with active components: the interaction energy of Caffeic acid and VEGFR2 protein was -7.5 kcal/mol, the interaction energy of Ferulic acid and VEGFR2 protein was -7.8 kcal/mol, the interaction energy of Ligustilide and VEGFR2 protein was -8.0 kcal/mol, the interaction energy of Senkyunolide A and VEGFR2 protein was -7.7 kcal/mol.

CX Extract Promotes VEGFR2 Protein Phosphorylation in Theca Layers of Preovulatory Follicles

VEGFR2 is a receptor that could bind to VEGFA. Increased expression of phosphorylated VEGFR2 can promote angiogenesis. The expression of VEGFR2 in theca layers of preovulatory follicles (F1–F3) was detected by western blot. The results showed that the phosphorylation levels of VEGFR2 in the F1 to F3 theca layers at 35 wk were higher expression than those at 75 wk ($P < 0.001$). CX extract significantly increased the phosphorylation levels of VEGFR2 in the F1 to F3 theca layers at treatment groups compared to 75 wk ($P < 0.05$, $P < 0.01$, and $P < 0.001$) (Figure 4A–C). We measured the expression of CD31 in the F1 to F3 theca layers. The results showed that the levels of the protein levels of

CD31 in the F1 to F3 theca layers at 35 wk were higher expression than those at 75 wk ($P < 0.001$). Compared with 75 wk, CX extract significantly increased the levels of VEGFR2 in F1 to F3 theca layers at treatment groups ($P < 0.05$, $P < 0.01$, and $P < 0.001$). As shown in Figure 4D, E, and F, IF results show that the phosphorylation levels of VEGFR2 in F1 to F3 theca layers at 35 wk were higher expression than those at 75 wk. The phosphorylation levels of VEGFR2 in groups 75 wk + L, 75 wk + M, and 75 wk + H were up-regulated more than in group 75 wk. Furthermore, the expression levels of VEGFR2 did not increase significantly in each group (Figure 4G–I).

CX Extract Promotes HIF1 α and VEGF Protein Expression in Granulosa Layers of Preovulatory Follicles

VEGFA plays a role in promoting angiogenesis. HIF1 α is a transcription factor induced by hypoxia and a potent inducer of VEGFA. The expression of HIF1 α and VEGFA in granulosa layers of preovulatory follicles (F1–F3) were detected by Western blot. The protein levels of VEGFA and HIF1 α in F1 to F3 granulosa layers at 35 wk were higher expressed than those at 75 wk ($P < 0.001$). CX extract significantly up-regulated the protein levels of HIF1 α and VEGFA in F1 to F3

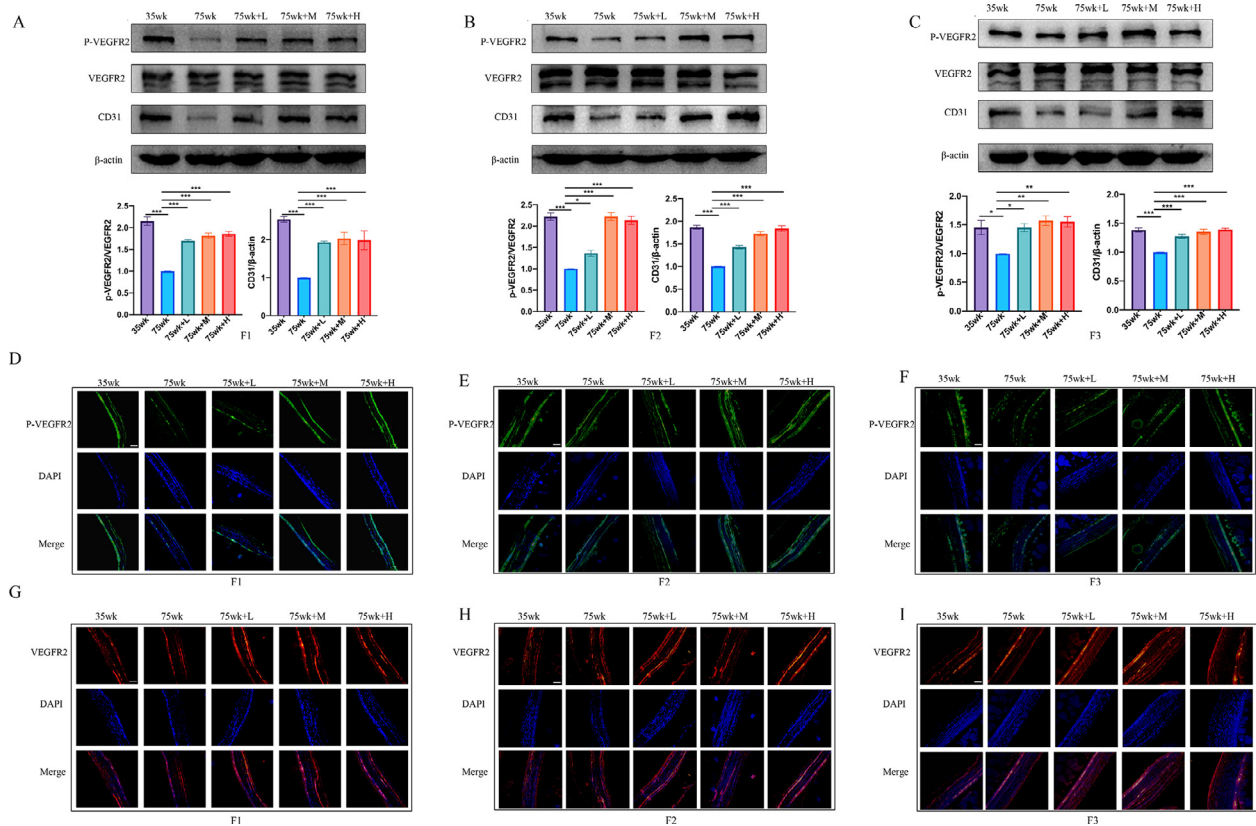


Figure 4. Dose-dependent effects of CX extract on theca layers in preovulatory follicles of late-phase laying hens. (A), (B), and (C) Western blot to detect the expression of P-VEGFR2, VEGFR2 and CD31 in F1 (A), F2 (B) and F3 (C) theca layers after CX extract treated, quantified according to the western blot. β -actin was included as a loading control. (D), (E), and (F) Immunofluorescence staining of P-VEGFR2 in CX extract-treated F1 (D), F2 (E), and F3 (F). Scale bar = 100 μ m. (G), (H), and (I) Immunofluorescence staining of VEGFR2 in CX extract-treated F1 (G), F2 (H), and F3 (I). Scale bar = 100 μ m. All experiments were performed in triplicate, and the data are the mean \pm S.E.M (* P < 0.05, ** P < 0.01, *** P < 0.001).

granulosa layers at CX extract treatment groups compared to 75 wk (P < 0.05, P < 0.01, and P < 0.001) (Figure 5A–C). As shown in Figure 5D–F, IF results show that HIF1 α is mainly expressed in granulosa layers. The protein levels of HIF1 α in F1 to F3 granulosa layers at 35 wk were higher expressed than those at 75 wk, and the protein levels of HIF1 α in groups 75 wk + L, 75 wk + M, and 75 wk + H were up-regulated compared to group 75 wk. As the IF results showed that the protein levels of VEGFA in F1 to F3 granulosa layers at 35 wk were higher expressed than those at 75 wk, and the protein levels of VEGFA in groups 75 wk + L, 75 wk + M, and 75 wk + H were up-regulated compared to those in group 75 wk (Figure 5G–I).

Effects of CX Extract on PI3K/AKT and RAS/ERK Signaling Pathway in FMECs

In order to clarify the mechanism of CX extract promoting angiogenesis in preovulatory follicles, we isolated FMECs from the theca layers. Cck-8 was used to detect the effect of CX extract on the proliferation of FMECs. As the results were shown in Figure S2 A, FMECs proliferated most at 100 and 200 μ g/mL concentrations of CX extract. PI3K/AKT and RAS/RAF signaling pathways are associated with cell proliferation, migration and angiogenesis. As shown in Figure 6A, western blot

results showed that CX extract could effectively activate the phosphorylation levels of PI3K, AKT, MTOR, and P70S6K in FMECs (P < 0.05, P < 0.01, and P < 0.001). Compared with the control group, CX extract significantly up-regulated the protein levels of RAS and RAF and increased the phosphorylation levels of MEK and ERK in FMECs (P < 0.05, P < 0.01, and P < 0.001) (Figure 6B). As shown in Figure 6C, the phosphorylation levels of VEGFR2 in FMECs after CX extract treatment were higher than in the control group (P < 0.05, P < 0.001). FMECs invasion metastasis is due to the hydrolysis of secretion of MMPs. Western blot was used to detect MMP2 and MMP9 protein levels (Figure 6D). Compared with the control group, CX extract significantly up-regulated the protein level of MMP2 and MMP9 (P < 0.05, P < 0.01). As IF staining showed, the phosphorylation levels of VEGFR2 in FMECs were higher than those in the control group, and the protein levels of VEGFR2 had no significant difference from those groups (Figure 6E, F).

CX Extract Promotes FMECs Invasion, Migration, and Tube Forming

Transwell invasion, wound healing, and tube forming experiments were used to determine the effect of CX extract on the ability of invasion, migration and

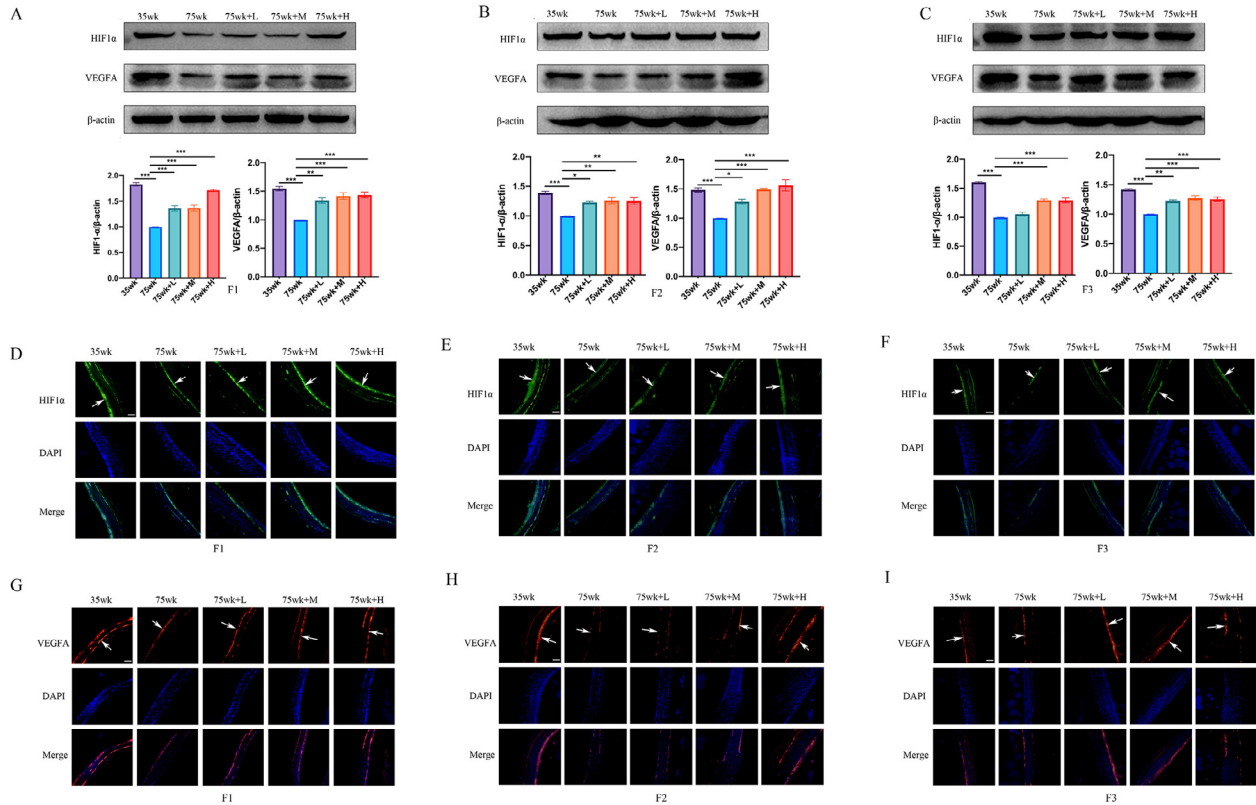


Figure 5. Dose-dependent effects of CX extract on granulosa layer in preovulatory follicles of late-phase laying hens. (A), (B), and (C) Western blot to detect the expression of HIF1 α and VEGFA in F1 (A), F2 (B), and F3 (C) granulosa layers after CX extract treated, quantified according to the western blot. β -actin was included as a loading control. (D), (E), and (F) Immunofluorescence staining of HIF1 α in CX extract-treated F1 (D), F2 (E), and F3 (F). Scale bar = 100 μ m. The white arrows refer to granulosa layers. (G), (H), and (I) Immunofluorescence staining of VEGFA in CX extract-treated F1 (G), F2 (H), and F3 (I). Scale bar = 100 μ m. The white arrows refer to granulosa layers. All experiments were performed in triplicate, and the data are the mean \pm S.E.M (* P < 0.05, ** P < 0.01, *** P < 0.001).

vascular formation in FMECs. As Figure 7A and B shown, compared with the control group, the invasion ability of FMECs treated with CX extract was significantly enhanced (P < 0.05, P < 0.01). The effect of CX extract on the migration of FMECs was detected by the wound healing assay (Figure 7C, and D). The migration distances in the CX extract treated groups were increased obviously than those in the control group at 6 h (P < 0.001). In particular, FMECs at 200 μ g/mL concentrations of CX extract had already overgrown in the “wound” at 12 h. Matrigel was used to simulate the environment of blood vessel formation in vivo (Figure 7E and F). Compared with the control group, the number of master junctions and total length increased significantly in the CX extract treated groups (P < 0.05, P < 0.01). The results showed that CX extract treated groups observed a better capillary network.

CX Extract Promotes Expression of VEGFA in GCs through PI3K/AKT and RAS/ERK Signaling Pathway

In this study, we isolated GCs from the granulosa layer. GCs in preovulatory follicles simulate HIF1 α expression through the conduction of signal pathways, promote the secretion of VEGFA, and thus promote

angiogenesis in preovulatory follicles. The PI3K/AKT and RAS/ERK signaling pathways are effective signal pathways to activate HIF1 α expression. As the results are shown in Figure S2 B, GCs proliferated most at 100 and 200 μ g/mL concentrations of CX extract. As shown in Figure 8A, western blot result showed that CX extract could effectively activate the phosphorylation levels of PI3K, AKT, MTOR and P70S6K in GCs (P < 0.05, P < 0.01, and P < 0.001). Compared with the control group, CX extract significantly up-regulated the protein levels of RAS and RAF and increased the phosphorylation levels of MEK and ERK in GCs in CX extract treatment groups (P < 0.05, P < 0.01, and P < 0.001) (Figure 8B). The results show that the protein level of HIF1 α and VEGFA increased significantly in GCs treated by CX extract (P < 0.05, P < 0.001) (Figure 8C). We performed IF experiments in order to prove that CX extract promotes the expression of HIF1 α and VEGFA. As shown in Figure 8D and E, the protein HIF1 α and VEGFA were expressed in the nucleus of GCs. CX extract increased HIF1 α and VEGFA expression in 100 and 200 μ g/mL CX extract treatment groups. In this study, we used Elisa to prove that CX extract promotes the secretion of VEGFA in GCs. As the results showed, the GCs of CX treated groups secreted more VEGFA in medium than those in the control group (P < 0.05) (Figure 8F). To further

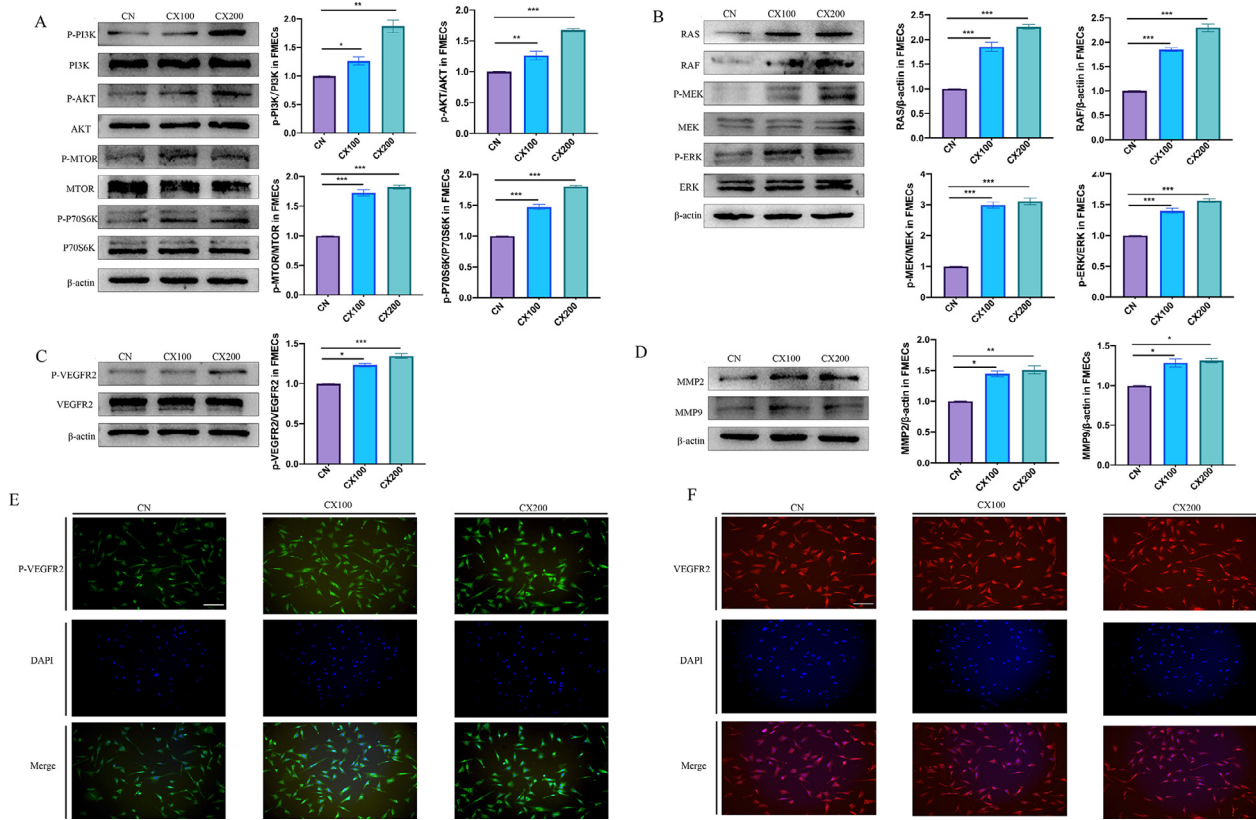


Figure 6. Effect of CX extract on PI3K/AKT and RAS/ERK signaling pathway, and MMPs proteins levels in FMECs. (A) Western blot to detect the expression of PI3K/AKT signaling pathway in FMECs after CX extract treated, quantified according to the western blot. β -actin was included as a loading control. (B) Western blot to detect the expression of RAS/ERK signaling pathway in FMECs after CX extract treated, quantified according to the western blot. β -actin was included as a loading control. (C) Western blot to detect the expression of P-VEGFR2 and VEGFR2 in FMECs after CX extract treated, quantified according to the western blot. β -actin was included as a loading control. (D) Western blot to detect the expression of MMP2 and MMP9 in FMECs after CX extract treated, quantified according to the western blot. β -actin was included as a loading control. (E) Immunofluorescence staining of P-VEGFR2 in CX extract-treated FMECs. Scale bar = $100\mu\text{m}$. (F) Immunofluorescence staining of VEGFR2 in CX extract-treated FMECs. Scale bar = $100\mu\text{m}$. All experiments were performed in triplicate, and the data are the mean \pm S.E.M (* $P < 0.05$, ** $P < 0.01$, *** $P < 0.001$).

prove the connection between GCs and FMECs, we added the medium (control groups of GCs and CX treated groups of GCs) to FMECs, respectively, and then FMECs were seeded in Matrigel. Compared with the control group, the number of master junctions and total length increased significantly in the CX extract treated groups ($P < 0.05$, $P < 0.01$) (Figure 8G).

DISCUSSION

The organism vascular system, with the exception of wound healing and some pathological processes, such as neoplasia, is often dormant. This is not the situation in the ovary, where the growth of follicles, ovulation, and the subsequent creation of the corpus luteum are marked by strong angiogenesis and enhanced blood vessel permeability Fraser and Duncan (2005). The ovary is an uncommon and very important tissue for research on the physiological and pathological regulation of blood vessel growth since it is practically certain that various types of ovarian dysfunction are linked to anomalies in the angiogenic process (Di Pietro et al., 2018; He et al., 2018; Zhou et al., 2021). The vascular network of the preovulatory follicle is extensive. The discovery of

endothelial cells in ovarian sections, however, demonstrates that primordial follicles lack a separate vascular supply (Shimizu et al., 2012). Therefore, to support the rapidly growing follicle, angiogenesis must continue and a capillary network must be developed. It is crucial to maintain an abundant vascular network in preovulatory follicles since commercial laying chickens can lay more than 320 eggs each year (Kim et al., 2016). An abundant vascular network is convenient for uptake of large amounts of vitellogenin and very-low-density lipoprotein (VLDL) in laying hens. In this study, we provided CX extract to late-phase laying hens, and the results demonstrated that CX extract might stimulate preovulatory follicle angiogenesis in vivo (Figure 1C). CD31 is a specific marker of blood vessels. Through IF staining, we found that the expression of CD31 in preovulatory follicles increased significantly in the CX treatment group (Figure 1H–J). We used LC-MS to identify the CX extract's constituent parts, and network pharmacology to assess the parts and predicted targets in order to further investigate the impact of CX extract on the angiogenesis of preovulatory follicles in late-phase laying hens.

CX may now be shown to have certain effects on hemorheology, hemodynamics, platelet functions, microcirculation functions, dilation of blood vessels and

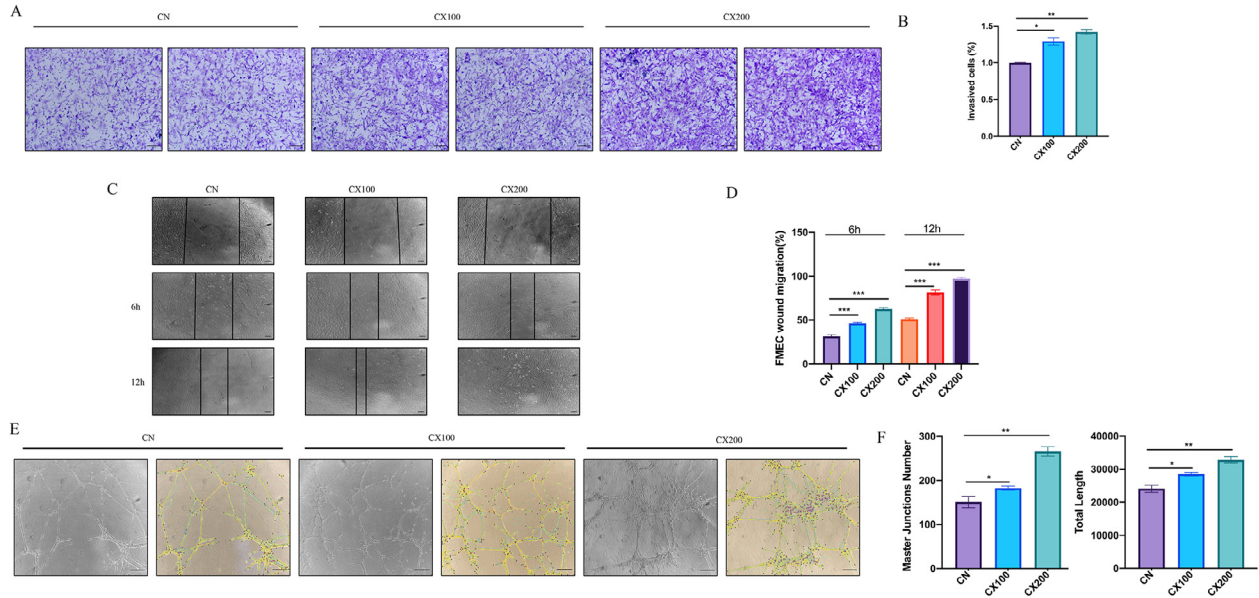


Figure 7. Effect of CX extract on invasion, migration and tube form ability of FMECs. (A and B) FMECs treated with CX extract were seeded in Transwell chamber, ECG medium was added in the lower chamber, and the number of cells passing through Transwell chamber was calculated after incubation for 24 h. Scale bar = 100 μ m. (C and D) Cells migration ability of different groups were measured by wound healing. Photographs from 0 h to 6 h and 12 h of the scratch were taken to measure the percentage of cell migration. Scale bar = 100 μ m. (E and F) Photographs of capillary-like structures in different groups of cells after the addition of CX extract were shown. Image J software is used to measure the capillary network. Histograms, respectively, on behalf of the number of master junctions and total length. Scale bar = 100 μ m. All experiments were performed in triplicate, and the data are the mean \pm S.E.M (* P < 0.05, ** P < 0.01, *** P < 0.001).

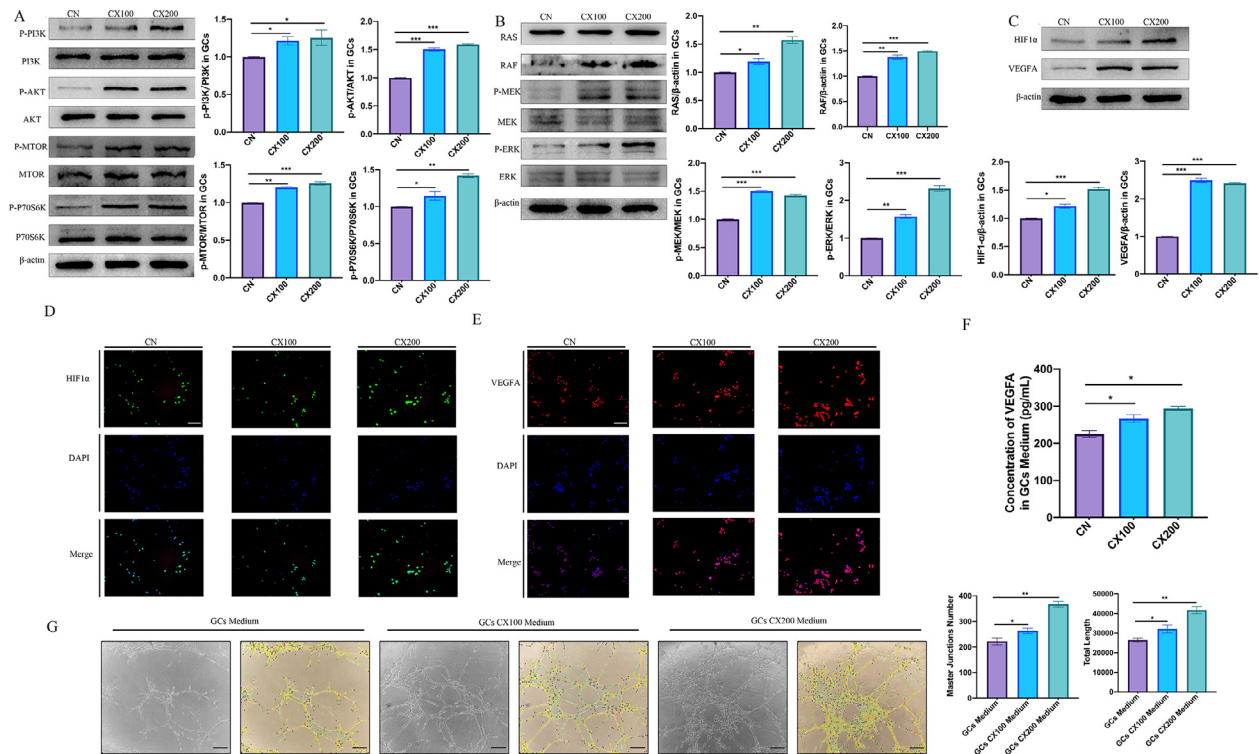


Figure 8. Effect of CX extract on PI3K/AKT and RAS/ERK signaling pathway, HIF1 α and VEGFA proteins levels in GCs. (A) Western blot to detect the expression of PI3K/AKT signaling pathway in GCs after CX extract treated, quantified according to the western blot. β -actin was included as a loading control. (B) Western blot to detect the expression of RAS/ERK signaling pathway in GCs after CX extract treated, quantified according to the western blot. β -actin was included as a loading control. (C) Western blot to detect the expression of HIF1 α and VEGFA in GCs after CX extract treated, quantified according to the western blot. β -actin was included as a loading control. (D) Immunofluorescence staining of HIF1 α in CX extract-treated GCs. Scale bar = 100 μ m. (E) Immunofluorescence staining of VEGFA in CX extract-treated GCs. Scale bar = 100 μ m. (F) Elisa to detect the concentration of VEGFA in GCs medium (pg/mL) after CX extract treated. (G) Photographs of capillary-like structures in different groups of FMECs after the addition of GCs mediums (CX extract treated) were shown. Image J software is used to measure the capillary network. Histograms, respectively, on behalf of the number of master junctions and total length. Scale bar = 100 μ m. All experiments were performed in triplicate, and the data are the mean \pm S.E.M (* P < 0.05, ** P < 0.01, *** P < 0.001).

angiogenesis, according to research findings (Zhou et al., 2016; Wang et al., 2011; Chen et al., 2020; Yang et al., 2020; Yang et al., 2021). CX is a natural plant that has intricate chemical constituents. More than 170 chemicals have been identified from CX since the 1970s (Pu et al., 2022). Modern separation technology has advanced, and it is now commonly accepted that one piece of material cannot adequately represent the quality of a CX. By using HPLC-UV technology, Yan et al. confirmed 12 components of CX, including Ligustrazine, Isoleucine, Caffeic acid, Ferulic acid, Isovanillin, Senkyunolide A, Ligustilide, Levistilide A (Yan et al., 2005). Ligustrazine has been demonstrated to promote peritoneal angiogenesis via modulating the VEGF/HIPPO/YAP signaling pathway (Zhu et al., 2021), while Ferulic acid does the same through VEGFA, PDGF, and HIF1 α enhanced angiogenesis (Lin et al., 2010). Ligustilide protects by enhancing angiogenesis following cerebral ischemia (Ren et al., 2020), and Caffeic acid helps arthritis while also stimulating angiogenesis (Fikry et al., 2019). It is challenging to fully define CX's potential mode of action because it includes a range of effective compounds that might promote angiogenesis. By combining the prediction targets of each compound with the targets of angiogenesis using network pharmacology, we are able to identify the effective CX components that support angiogenesis and identify their probable mechanisms (Shi et al., 2019). The findings of our research demonstrated that all of the chosen gene targets were associated with angiogenesis, and VEGFR2 (KDR) and HIF1 α were related to angiogenesis. According to the results of the go enrichment analysis, angiogenesis was connected to a number of biological processes, cellular elements, molecular activities, and signal pathways. In order to further explore the effect of CX on the angiogenesis of preovulatory follicles, we conducted a series of experiments in vivo and in vitro combined with the results of network pharmacology.

The preovulatory follicle theca layer, which is separated from the avascular granulosa layer by a specialized basement membrane, is where the capillary network develops. Endothelial cells from the blood vessels in the nearby ovarian stroma are recruited to the theca layer as the preovulatory follicles continue to develop. In the theca layer, endothelial cells make up half of the proliferating cells (Wulff et al., 2001; Kim et al., 2016). Numerous regulatory molecules interact in a complicated way throughout this process, with the VEGF family playing a prominent role. VEGF was initially identified as a vascular permeability factor when it was found (Dvorak, 2002). VEGFR1 (Flt-1) and VEGFR-2 are two tyrosine kinase receptors that VEGF acts on to stimulate the proliferation of vascular endothelial cells (Simons et al., 2016). In contrast to the theca layer, where angiogenesis occurs, VEGF is mostly synthesized in the latter stages of preovulatory follicles development in the avascular granulosa layer (Taylor et al., 2004). The VEGF receptors are expressed in endothelial cells of theca layers. HIF1 α has a significant role as a transcriptional regulator of VEGFA in many tissues and

physiological settings (Semenza, 2014). Although hypoxia is typically thought of as the primary regulator of HIF1 activity, it can also be regulated by processes that are not dependent on oxygen (Hudson et al., 2002; Ke and Costa (2006)). In fact, it has been demonstrated that both in vivo and in vitro, HIF1 α is necessary for LH regulated VEGFA expression (van den Driesche et al., 2008; Kim et al., 2009; Rico et al., 2014). In this study, we used western blot, IF and Elisa to prove that CX extract can increase the phosphorylation of VEGFR2 and the expression of CD31 in the preovulatory follicles theca layer of late-phase laying hens and promote the expression of HIF1 and VEGFA in the granulosa layer. Finally, it effectively promotes angiogenesis in preovulatory follicles (F1–F3).

A crucial regulator of angiogenesis is PI3K Claesson-Welsh and Welsh (2013). VEGFA activates PI3K via multiple pathways, including FAK (Sun et al., 2019), SHB (Holmqvist et al., 2004), GAB1 (Dance et al., 2006), IQGAP1 (Meyer et al., 2008), and direct PI3K binding to pY1175 in VEGFR2 (Dayanir et al., 2001). In the PI3K downstream signaling pathway, AKT plays a significant role in the biology of VEGF regulated endothelial cells. There are three different isoforms of AKT that are present in endothelial cells and are activated by PI3K through PDK1 and MTORC2 (Ackah et al., 2005; Suzuki et al., 2007). Through endothelial cells tubule formation in vitro, survival, proliferation, vascular permeability, and the production and release of MMPs, active PI3K and AKT have been related to angiogenesis van Hinsbergh and Koolwijk (2008). The ERK pathway plays a crucial role in controlling cell development by relaying extracellular signals from ligand-bound cell surface tyrosine kinase receptors like VEGFR2 and transmitting them to the nucleus via a cascade of specialized phosphorylation events beginning with RAS activation (Sridhar et al., 2005). In this study, we first isolated FMECs from the theca layers of preovulatory follicles and discovered that CX extract could promote VEGFR2 phosphorylation and the expression of MMP2 and MMP9 in FMECs, as well as promote FMECs proliferation, invasion, migration, and tubule formation in vitro by activating the PI3K/AKT and RAS/ERK signaling pathways. Previous studies have demonstrated that elevated HIF1 α activity can control VEGFA expression in GCs (Alam et al., 2009; Rico et al., 2014). HIF1 α tends to accumulate in cells in nonhypoxic circumstances as a result of growth factors, cytokines, and other signaling molecules Masoud and Li (2015). Through the downstream component MTOR and AKT, PI3K controls protein synthesis. MTOR promotes the P70S6K phosphorylation and induces HIF1 α translation (Gingras et al., 2001). Certain growth factors activate RAS which in turn stimulates the RAS/RAF/MEK/ERK kinase cascade (Semenza, 2002). Activated ERK phosphorylates 4E-BP1, P70S6K, and MNK. The enhanced rate of mRNA translation into HIF-1 protein is the end effect of these signaling processes (Sang et al., 2003). Our results demonstrated that CX extract might stimulate the PI3K and RAS downstream proteins,

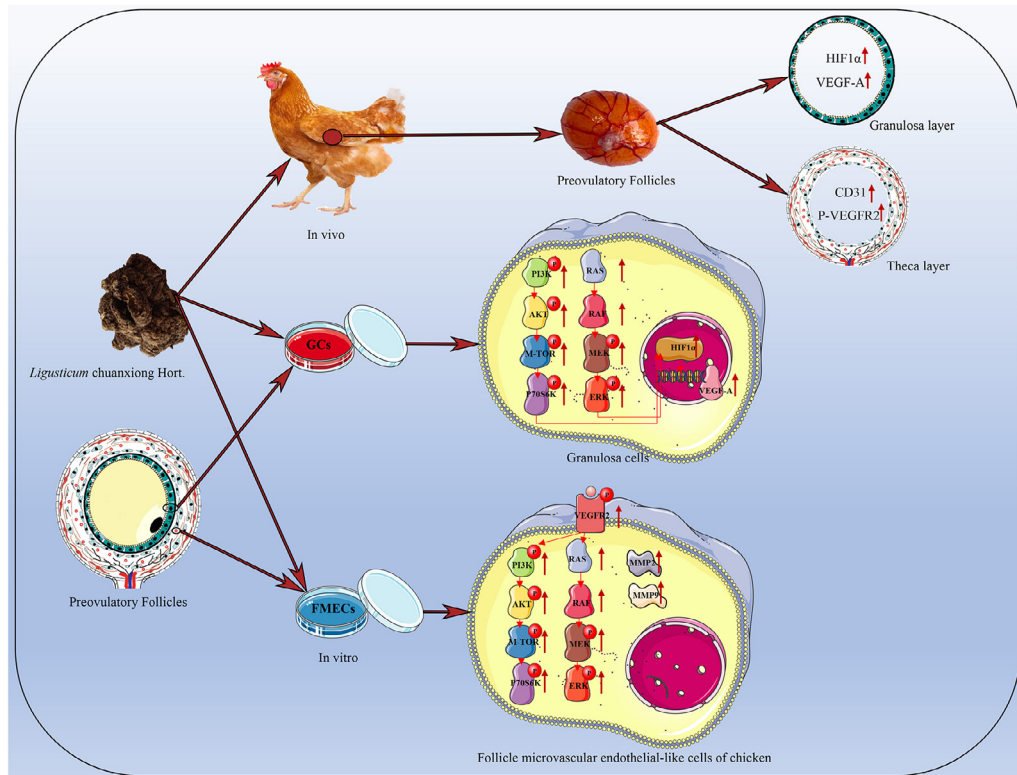


Figure 9. CX extract promotes angiogenesis of preovulatory follicles by up-regulation the expression of HIF1 α and VEGFA in granulosa layers and VEGFR2 in theca layers.

consequently boosting HIF1 α protein production and VEGFA secretion in GCs.

CONCLUSION

In conclusion, CX extract can increase the angiogenesis of preovulatory follicles (F1–F3) of late-phase laying hens. We verified that CX extract could promote VEGFR2 phosphorylation in preovulatory follicles theca layers and VEGFA secretion in granulosa layers of late-phase laying hens. The experimental results in vitro demonstrated that CX extract could up-regulate the phosphorylation level of VEGFR2 in FMECs and promote the proliferation, invasion and migration through PI3K/AKT and RAS/ERK signaling pathways. Moreover, CX extract could up-regulate the expression of HIF1 α in GCs through PI3K/AKT and RAS/ERK signaling pathways, thereby promoting the secretion of VEGFA (Figure 9). Our research deeply discussed the effects and mechanism of CX extract on the angiogenesis of preovulatory follicles in late-phase laying hens and provided some insights on the mechanism of synergistic effect of CX components on multiple targets, setting the stage for the design of functional animal feed for late-phase laying hens.

ACKNOWLEDGMENTS

This work was supported by the national key research and development plan of China under grant number 2017YFD0502200.

Consent for publication: Written informed consent for publication was obtained from all participants.

Authors' contributions: The work was mainly conceived and designed by Hao Chen, Jun Ma and Wenhui Yu; Hao Chen, Xin Chen, Zhenlei Ping and Lixue Fang performed the experiments; Hao Chen collected and analyzed experimental data; Xiaowen Jiang and Ming Ge managed the project; The manuscript was written by Hao Chen. All the authors read and approved the final manuscript.

Availability of data and materials: The datasets used and/or analyzed during the current study are available from the corresponding author on reasonable request.

DISCLOSURES

The authors have no conflicts of interest to declare.

SUPPLEMENTARY MATERIALS

Supplementary material associated with this article can be found, in the online version, at [doi:10.1016/j.psj.2022.102430](https://doi.org/10.1016/j.psj.2022.102430).

REFERENCES

- Ackah, E., J. Yu, S. Zoellner, Y. Iwakiri, C. Skurk, R. Shibata, N. Ouchi, R. M. Easton, G. Galasso, M. J. Birnbaum, K. Walsh, and W. C. Sessa. 2005. Akt1/protein kinase Balpha is critical for ischemic and VEGF-mediated angiogenesis. *J. Clin. Invest.* 115:2119–2127.

- Alam, H., J. Weck, E. Maizels, Y. Park, E. J. Lee, M. Ashcroft, and M. Hunzicker-Dunn. 2009. Role of the phosphatidylinositol-3-kinase and extracellular regulated kinase pathways in the induction of hypoxia-inducible factor (HIF)-1 activity and the HIF-1 target vascular endothelial growth factor in ovarian granulosa cells in response to follicle-stimulating hormone. *Endocrinology* 150:915–928.
- Apte, R. S., D. S. Chen, and N. Ferrara. 2019. VEGF in signaling and disease: beyond discovery and development. *Cell* 176:1248–1264.
- Chen, H., X. Chen, Z. Ping, X. Jiang, M. Ge, J. Ma, and W. Yu. 2022a. Promotion effect of angelica sinensis extract on angiogenesis of chicken preovulatory follicles in vitro. *Poult. Sci.* 101:101938.
- Chen, H., T. Nie, P. Zhang, J. Ma, and A. Shan. 2022b. Hesperidin attenuates hepatic lipid accumulation in mice fed high-fat diet and oleic acid induced HepG2 via AMPK activation. *Life Sci.* 296:120428.
- Chen, Z., L. Hu, Y. Liao, X. Zhang, Z. Yang, C. Hu, and L. Yu. 2020. Different processed products of curcuma radix regulate pain-related substances in a rat model of Qi stagnation and blood stasis. *Front. Pharmacol.* 11:242.
- Chen, Z., C. Zhang, F. Gao, Q. Fu, C. Fu, Y. He, and J. Zhang. 2018. A systematic review on the rhizome of *Ligusticum chuanxiong* Hort. (*Chuanxiong*). *Food Chem. Toxicol.* 119:309–325.
- Claesson-Welsh, L., and M. Welsh. 2013. VEGFA and tumour angiogenesis. *J. Intern. Med.* 273:114–127.
- Dance, M., A. Montagner, A. Yart, B. Masri, Y. Audigier, B. Perret, J. P. Salles, and P. Raynal. 2006. The adaptor protein Gab1 couples the stimulation of vascular endothelial growth factor receptor-2 to the activation of phosphoinositide 3-kinase. *J. Biol. Chem.* 281:23285–23295.
- Dayanir, V., R. D. Meyer, K. Lashkari, and N. Rahimi. 2001. Identification of tyrosine residues in vascular endothelial growth factor receptor-2/FLK-1 involved in activation of phosphatidylinositol 3-kinase and cell proliferation. *J. Biol. Chem.* 276:17686–17692.
- Di Pietro, M., N. Pascuali, F. Parborell, and D. Abramovich. 2018. Ovarian angiogenesis in polycystic ovary syndrome. *Reproduction* 155:R199–R209.
- Dong, X. L., W. X. Yu, C. M. Li, L. P. Zhou, and M. S. Wong. 2020. Chuanxiong (Rhizome of *Ligusticum chuanxiong*) protects ovariectomized hyperlipidemic rats from bone loss. *Am. J. Chin. Med.* 48:463–485.
- Dvorak, H. F. 2002. Vascular permeability factor/vascular endothelial growth factor: a critical cytokine in tumor angiogenesis and a potential target for diagnosis and therapy. *J. Clin. Oncol.* 20:4368–4380.
- Fikry, E. M., A. M. Gad, A. H. Eid, and H. H. Arab. 2019. Caffeic acid and ellagic acid ameliorate adjuvant-induced arthritis in rats via targeting inflammatory signals, chitinase-3-like protein-1 and angiogenesis. *Biomed. Pharmacother.* 110:878–886.
- Fraser, H. M., and W. C. Duncan. 2005. Vascular morphogenesis in the primate ovary. *Angiogenesis* 8:101–116.
- Gingras, A. C., B. Raught, and N. Sonenberg. 2001. Regulation of translation initiation by FRAP/mTOR. *Genes Dev.* 15:807–826.
- Hao, E. Y., D. H. Wang, Y. F. Chen, R. Y. Zhou, H. Chen, and R. L. Huang. 2021. The relationship between the mTOR signaling pathway and ovarian aging in peak-phase and late-phase laying hens. *Poult. Sci.* 100:334–347.
- He, Y., D. Chen, L. Yang, Q. Hou, H. Ma, and X. Xu. 2018. The therapeutic potential of bone marrow mesenchymal stem cells in premature ovarian failure. *Stem Cell Res. Ther.* 9:263.
- Holmqvist, K., M. J. Cross, C. Rolny, R. Hägerkvist, N. Rahimi, T. Matsumoto, L. Claesson-Welsh, and M. Welsh. 2004. The adaptor protein shb binds to tyrosine 1175 in vascular endothelial growth factor (VEGF) receptor-2 and regulates VEGF-dependent cellular migration. *J. Biol. Chem.* 279:22267–22275.
- Hudson, C. C., M. Liu, G. G. Chiang, D. M. Otterness, D. C. Loomis, F. Kaper, A. J. Giaccia, and R. T. Abraham. 2002. Regulation of hypoxia-inducible factor 1alpha expression and function by the mammalian target of rapamycin. *Mol. Cell. Biol.* 22:7004–7014.
- Ke, Q., and M. Costa. 2006. Hypoxia-inducible factor-1 (HIF-1). *Mol. Pharmacol.* 70:1469–1480.
- Kim, D., J. Lee, and A. L. Johnson. 2016. Vascular endothelial growth factor and angiopoietins during hen ovarian follicle development. *Gen. Comp. Endocrinol.* 232:25–31.
- Kim, J., I. C. Bagchi, and M. K. Bagchi. 2009. Signaling by hypoxia-inducible factors is critical for ovulation in mice. *Endocrinology* 150:3392–3400.
- Li, D., Y. Long, S. Yu, A. Shi, J. Wan, J. Wen, X. Li, S. Liu, Y. Zhang, N. Li, C. Zheng, M. Yang, and L. Shen. 2021. Research advances in cardio-cerebrovascular diseases of *Ligusticum chuanxiong* Hort. *Front. Pharmacol.* 12:832673.
- Lim, L. S., P. Shen, Y. H. Gong, and E. L. Yong. 2006. Dimeric progestins from rhizomes of *Ligusticum chuanxiong*. *Phytochemistry* 67:728–734.
- Lin, C. M., J. H. Chiu, I. H. Wu, B. W. Wang, C. M. Pan, and Y. H. Chen. 2010. Ferulic acid augments angiogenesis via VEGF, PDGF and HIF-1 alpha. *J. Nutr. Biochem.* 21:627–633.
- Liu, J. L., Q. J. Fan, S. L. Zheng, J. Tan, J. Zhou, J. C. Yuan, S. M. Yang, and F. L. Kong. 2014. Quantitative determination of 5 active ingredients in different harvest periods of *Ligusticum chuanxiong* by HPLC. *Zhongguo Zhong Yao Za Zhi* 39:1650–1655.
- Ma, Y., S. Zhou, X. Lin, W. Zeng, Y. Mi, and C. Zhang. 2020. Effect of dietary N-carbamylglutamate on development of ovarian follicles via enhanced angiogenesis in the chicken. *Poult. Sci.* 99:578–589.
- Masoud, G. N., and W. Li. 2015. HIF-1 α pathway: role, regulation and intervention for cancer therapy. *Acta Pharm. Sin. B* 5:378–389.
- Meyer, R. D., D. B. Sacks, and N. Rahimi. 2008. IQGAP1-dependent signaling pathway regulates endothelial cell proliferation and angiogenesis. *PLoS One* 3:e3848.
- Nalbandov, A. V., and M. F. James. 1949. The blood-vascular system of the chicken ovary. *Am. J. Anat.* 85:347–377 incl 345 pl.
- Peach, C. J., V. W. Mignone, M. A. Arruda, D. C. Alcobia, S. J. Hill, L. E. Kilpatrick, and J. Woolard. 2018. Molecular pharmacology of VEGF-A isoforms: binding and signalling at VEGFR2. *Int. J. Mol. Sci.* 19:1264.
- Pu, Z. H., M. Dai, L. Xiong, and C. Peng. 2022. Total alkaloids from the rhizomes of *Ligusticum striatum*: a review of chemical analysis and pharmacological activities. *Nat. Prod. Res.* 36:3489–3506.
- Ren, C., N. Li, C. Gao, W. Zhang, Y. Yang, S. Li, X. Ji, and Y. Ding. 2020. Ligustilide provides neuroprotection by promoting angiogenesis after cerebral ischemia. *Neurol. Res.* 42:683–692.
- Rico, C., A. Dodelet-Devillers, M. Paquet, M. Tsoi, E. Lapointe, P. Carmeliet, and D. Boerboom. 2014. HIF1 activity in granulosa cells is required for FSH-regulated Vegfa expression and follicle survival in mice. *Biol. Reprod.* 90:135.
- Robinson, R. S., K. J. Woad, A. J. Hammond, M. Laird, M. G. Hunter, and G. E. Mann. 2009. Angiogenesis and vascular function in the ovary. *Reproduction* 138:869–881.
- Sang, N., D. P. Stiehl, J. Bohensky, I. Leshchinsky, V. Srinivas, and J. Caro. 2003. MAPK signaling up-regulates the activity of hypoxia-inducible factors by its effects on p300. *J. Biol. Chem.* 278:14013–14019.
- Scanes, C. G., H. Mozelic, E. Kavanagh, G. Merrill, and J. Rabii. 1982. Distribution of blood flow in the ovary of domestic fowl (*Gallus domesticus*) and changes after prostaglandin F-2 alpha treatment. *J. Reprod. Fertil.* 64:227–231.
- Semenza, G. 2002. Signal transduction to hypoxia-inducible factor 1. *Biochem. Pharmacol.* 64:993–998.
- Semenza, G. L. 2014. Hypoxia-inducible factor 1 and cardiovascular disease. *Annu. Rev. Physiol.* 76:39–56.
- Shi, X. Q., S. J. Yue, Y. P. Tang, Y. Y. Chen, G. S. Zhou, J. Zhang, Z. H. Zhu, P. Liu, and J. A. Duan. 2019. A network pharmacology approach to investigate the blood enriching mechanism of Danggui buxue Decoction. *J. Ethnopharmacol.* 235:227–242.
- Shimizu, T., Y. Hoshino, H. Miyazaki, and E. Sato. 2012. Angiogenesis and microvasculature in the female reproductive organs: physiological and pathological implications. *Curr. Pharm. Des.* 18:303–309.
- Simons, M., E. Gordon, and L. Claesson-Welsh. 2016. Mechanisms and regulation of endothelial VEGF receptor signalling. *Nat. Rev. Mol. Cell Biol.* 17:611–625.
- Sridhar, S. S., D. Hedley, and L. L. Siu. 2005. Raf kinase as a target for anticancer therapeutics. *Mol. Cancer Ther.* 4:677–685.
- Sun, X., L. Meng, W. Qiao, R. Yang, Q. Gao, Y. Peng, and Z. Bian. 2019. Vascular endothelial growth factor A/Vascular endothelial growth factor receptor 2 axis promotes human dental pulp stem cell migration via the FAK/PI3K/Akt and p38 MAPK signalling pathways. *Int. Endod. J.* 52:1691–1703.

- Suzuki, A., K. Hamada, T. Sasaki, T. W. Mak, and T. Nakano. 2007. Role of PTEN/PI3K pathway in endothelial cells. *Biochem. Soc. Trans.* 35:172–176.
- Tamanini, C., and M. De Ambrogi. 2004. Angiogenesis in developing follicle and corpus luteum. *Reprod. Domest. Anim.* 39:206–216.
- Tang, F., Y. M. Yan, H. L. Yan, L. X. Wang, C. J. Hu, H. L. Wang, H. Ao, C. Peng, and Y. Z. Tan. 2021. Chuanxiangdiolides R4 and R5, phthalide dimers with a complex polycyclic skeleton from the aerial parts of *Ligusticum chuanxiong* and their vasodilator activity. *Bioorg. Chem.* 107:104523.
- Taylor, P. D., S. G. Hillier, and H. M. Fraser. 2004. Effects of GnRH antagonist treatment on follicular development and angiogenesis in the primate ovary. *J. Endocrinol.* 183:1–17.
- Uemura, A., M. Fruttiger, P. A. D'Amore, S. De Falco, A. M. Joussen, F. Sennlaub, L. R. Brunck, K. T. Johnson, G. N. Lambrou, K. D. Rittenhouse, and T. Langmann. 2021. VEGFR1 signaling in retinal angiogenesis and microinflammation. *Prog. Retin. Eye Res.* 84:100954.
- van den Driesche, S., M. Myers, E. Gay, K. J. Thong, and W. C. Duncan. 2008. HCG up-regulates hypoxia inducible factor-1 alpha in luteinized granulosa cells: implications for the hormonal regulation of vascular endothelial growth factor A in the human corpus luteum. *Mol. Hum. Reprod.* 14:455–464.
- van Hinsbergh, V. W., and P. Koolwijk. 2008. Endothelial sprouting and angiogenesis: matrix metalloproteinases in the lead. *Cardiovasc. Res.* 78:203–212.
- Wang, W. R., R. Lin, H. Zhang, Q. Q. Lin, L. N. Yang, K. F. Zhang, and F. Ren. 2011. The effects of Buyang Huanwu Decoction on hemorheological disorders and energy metabolism in rats with coronary heart disease. *J. Ethnopharmacol.* 137:214–220.
- Wu, S., N. Wang, J. Li, G. Wang, S. W. Seto, D. Chang, and H. Liang. 2019. Ligustilide ameliorates the permeability of the blood-brain barrier model in vitro during oxygen-glucose deprivation injury through HIF/VEGF pathway. *J. Cardiovasc. Pharmacol.* 73:316–325.
- Wulff, C., S. J. Wiegand, P. T. Saunders, G. A. Scobie, and H. M. Fraser. 2001. Angiogenesis during follicular development in the primate and its inhibition by treatment with truncated Flt-1-Fc (vascular endothelial growth factor Trap(A40)). *Endocrinology* 142:3244–3254.
- Yan, R., S. L. Li, H. S. Chung, Y. K. Tam, and G. Lin. 2005. Simultaneous quantification of 12 bioactive components of *Ligusticum chuanxiong* Hort. by high-performance liquid chromatography. *J. Pharm. Biomed. Anal.* 37:87–95.
- Yang, J., R. Wang, X. Cheng, H. Qu, J. Qi, D. Li, Y. Xing, Y. Bai, and X. Zheng. 2020. The vascular dilatation induced by Hydroxysafflor yellow A (HSYA) on rat mesenteric artery through TRPV4-dependent calcium influx in endothelial cells. *J. Ethnopharmacol.* 256:112790.
- Yang, K., L. Zeng, A. Ge, Y. Chen, S. Wang, X. Zhu, and J. Ge. 2021. Exploring the regulatory mechanism of hedysarum multijugum maxim.-chuanxiong rhizoma compound on HIF-VEGF pathway and cerebral ischemia-reperfusion injury's biological network based on systematic pharmacology. *Front. Pharmacol.* 12:601846.
- Yang, X., X. Zeng, and T. Wu. 2010. Chuanxiong preparations for preventing stroke. *Cochrane Database Syst. Rev.* 20:Cd006765.
- Zhang, J., Q. Chen, D. Du, T. Wu, J. Wen, M. Wu, Y. Zhang, W. Yan, S. Zhou, Y. Li, Y. Jin, A. Luo, and S. Wang. 2019. Can ovarian aging be delayed by pharmacological strategies? *Aging (Albany NY)* 11:817–832.
- Zhou, F., Y. Song, X. Liu, C. Zhang, F. Li, R. Hu, Y. Huang, W. Ma, K. Song, and M. Zhang. 2021. Si-Wu-Tang facilitates ovarian function through improving ovarian microenvironment and angiogenesis in a mouse model of premature ovarian failure. *J. Ethnopharmacol.* 280:114431.
- Zhou, Y., M. Xie, Y. Song, W. Wang, H. Zhao, Y. Tian, Y. Wang, S. Bai, Y. Zhao, X. Chen, and G. She. 2016. Two traditional chinese medicines curcumae radix and curcumae rhizoma: an ethnopharmacology, phytochemistry, and pharmacology review. *Evid. Based Complement. Alternat. Med.* 2016:4973128.
- Zhu, X., Y. Shan, M. Yu, J. Shi, L. Tang, H. Cao, and M. Sheng. 2021. Tetramethylpyrazine ameliorates peritoneal angiogenesis by regulating VEGF/Hippo/YAP signaling. *Front. Pharmacol.* 12:649581.